

RESEARCH

Accuracy of zoomed digital image in the detection of periodontal bone defect: *in vitro* study

JAND de Moraes¹, CE Sakakura¹, LCM Loffredo² and G Scaf^{*1}

¹Department of Oral Diagnosis and Surgery, Araraquara Dental School, State of São Paulo University, Unesp, Araraquara, São Paulo, Brazil; ²Department of Social Dentistry, Araraquara Dental School, State of São Paulo University, Unesp, Araraquara, São Paulo, Brazil

Objectives: (1) To evaluate the intraobserver agreement related to image interpretation and (2) to compare the accuracy of 100%, 200% and 400% zoomed digital images in the detection of simulated periodontal bone defects.

Methods: Periodontal bone defects were created in 60 pig hemi-mandibles with slow-speed burs 0.5 mm, 1.0 mm, 1.5 mm, 2.0 mm and 3.0 mm in diameter. 180 standardized digital radiographs were made using Schick sensor and evaluated at 100%, 200% and 400% zooming. The intraobserver agreement was estimated by Kappa statistic (κ). For the evaluation of diagnostic accuracy receiver operating characteristic (ROC) analysis was performed followed by chi-square test to compare the areas under ROC curves according to each level of zooming.

Results: For 100%, 200% and 400% zooming the intraobserver agreement was moderate ($\kappa = 0.48$, $\kappa = 0.54$ and $\kappa = 0.43$, respectively) and there were similar performances in the discrimination capacity, with ROC areas of 0.8611 (95% CI: 0.7660–0.9562), 0.8600 (95% CI: 0.7659–0.9540), and 0.8368 (95% CI: 0.7346–0.9390), respectively, with no statistical significant differences (χ^2 -test; $P = 0.8440$).

Conclusions: A moderate intraobserver agreement was observed in the classification of periodontal bone defects and the 100%, 200% and 400% zoomed digital images presented similar performances in the detection of periodontal bone defects.

Dentomaxillofacial Radiology (2006) **35**, 139–142. doi: 10.1259/dmfr/31981949

Keywords: dental radiography; digital radiography; radiographic zooming; alveolar bone loss; agreement; accuracy

Introduction

Radiographic examinations are considered a useful diagnostic aid to detect bone loss originating from periodontal disease. However, there are limitations due to the two-dimensional imaging representation of the alveolar bone.¹ Although radiographic imaging is very often used to verify the existence, extent and location of periodontal disease,² there also needs to be substantial amount of mineral loss (30–50%) before bone loss can be detected.³

The advance of digital imaging in dentistry has been an alternative to film-based imaging. Digital processing and image manipulation may enhance diagnostic interpretation. One advantage of digital imaging is the ability to manipulate the image using brightness and contrast control, colorization, inversion and zooming tools in

order to enhance the diagnosis for detection of lesions during interpretation.^{4–7}

The zooming function comes in a software for image magnification or reduction⁸ and in some studies has been shown to provide improvement of the diagnosis efficacy of initial caries lesions^{9,10} and detection of small endodontic files in relation to the radiographic apex.¹¹ However, the digital magnification did not affect the detection of root fractures¹² and both Moystad et al¹³ and Scaf et al⁹ showed the limitation of zoomed digital function for radiographic interpretation of caries lesions.

In order to determine the improvement of periodontal bone defect detection by this digital tool, the aims of this study were: (1) to evaluate the intraobserver agreement related to image interpretation and (2) to compare the accuracy of 100%, 200% and 400% zoomed digital images in the detection of simulated periodontal bone defects.

*Correspondence to: Dr Gulnara Scaf, Rua Humaitá, 1680, 14801-903, Araraquara, São Paulo, Brazil; E-mail: scaf@foar.unesp.br
Received 3 August 2004; revised 14 June 2005; accepted 12 July 2005

Materials and methods

Sample size

Sixty hemi-mandibles from different pigs were used. Initially 240 images were obtained where 60 images were zoomed at each of the following levels: 100%, 200%, 400% and 804%. However, the level at 804% zooming was excluded from the analysis due to a limitation in the detection of periodontal bone defect. Thus, the material consisted of 180 zoomed images at 100%, 200% and 400%.

Bone defects

Periodontal bone defects were created in the most coronal portion of the interproximal buccal cortical plate between first and second premolar area in the lingual direction by removal of bone with slow-speed round burs corresponding to 0.5 mm, 1.0 mm, 1.5 mm, 2.0 mm and 3.0 mm in diameter, adapted from Stassinakis *et al.*¹⁴ Sixty periodontal defects were created, 12 of each diameter. For the purpose of the diagnostic accuracy analysis, due to a tendency for images of periodontal bone defect of 2.0 mm and 3.0 mm to score better for the presence of defect than 0.5 mm, 1.0 mm and 1.5 mm, they were classified as “bone defect” and “no bone defect”, with prevalence of 24/60 and 36/60, respectively.

Image acquisition

Digital images were acquired using Schick[®] equipment (Schick Technologies Inc., Long Island, NY) version 2.0. The sensor and hemi-mandible were stabilized with a fixing device. The digital radiographs were taken with the vertical long axis of the hemi-mandible fixed perpendicular to the central ray and parallel to the sensor at 70 cm focal-spot to object distance, including a 2.0 cm wooden block to simulate soft tissue. The X-ray unit (GE 1000; General Electric, Milwaukee, WI) was operated at 70 kVp, 10 mA and 18 impulses (Figure 1).

The image resolution was 635 ppi as size of the image was 900 × 641 dpi and the size of the pixel was 40 μm.¹⁵ The images were stored in the TIFF format (Tagged Image File Format) without compression (8 bits with resolution of 600 dpi, a file of about 700 KB).

Image manipulation

The images were manipulated with the aid of Schick[®] software version 2.0 running in a PC with 550 MHz processor (Pentium III; Intel, USA) 512 K, 129 Mb and Windows 98 operating system (Microsoft, USA) displayed on a 17" S-VGA flat screen monitor (1024 × 768 pixel resolution). Before zooming procedure, the brightness and contrast of all images were automatically adjusted.

Image interpretation

A radiologist experienced in using pig mandibles as experimental model did the radiographic interpretation. In order to minimize bias the radiologist was calibrated prior to undertaking the project. The readings were done twice on two different occasions independently and under blind conditions. The interval between the two readings

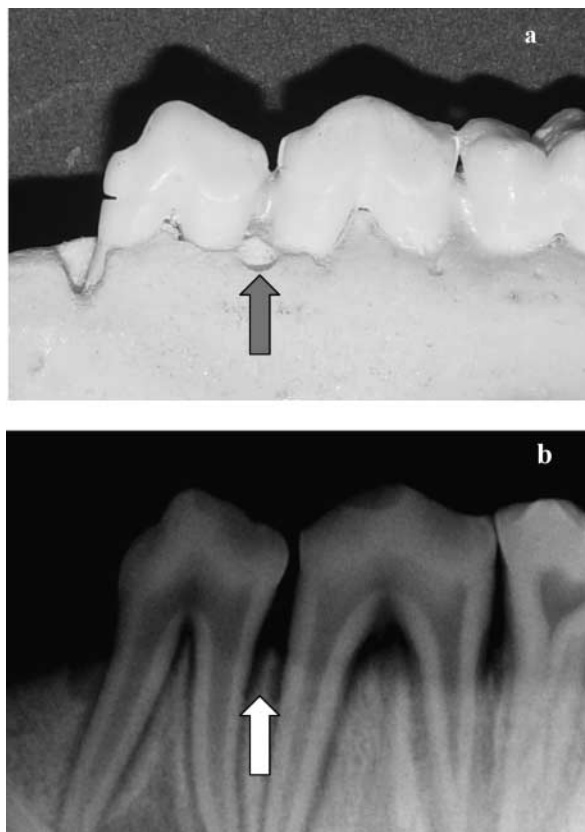


Figure 1 (a) Bone defect in dry pig hemi-mandible created with 3.0 mm round bur and (b) digital radiograph of the specimen

was 15 days. The sequence of image interpretation was done at random. The images were scored using a 5-point confidence scale to assess the periodontal bone defect as: 1 = definitely absent; 2 = probably absent; 3 = uncertain; 4 = probably present; 5 = definitely present. The observer read the images under reduced room light and viewing distance from 50 cm to 70 cm from the screen.

Statistical analysis

The intraobserver agreement was assessed using measures of observed agreement, expected agreement, Kappa statistic (κ) and 95% confidence interval.¹⁶ Kappa value (κ) was classified according to the standards proposed by Landis and Koch.¹⁷ In order to evaluate diagnostic procedures related to zoomed digital function for image interpretation, ROC analysis was performed on the basis of the datasets on the confidence rank scale, resulting in three ROC curves, and the differences in the areas were evaluated by χ^2 -test for correlated data.¹⁸ As reference-standard examination the defect sizes of 0.5 mm, 1.0 mm and 1.5 mm were considered as “no bone defect” while sizes of 2.0 mm and 3.0 mm as “bone defect”.

STATA statistical software, release 8.0 (Stata Corp., College Station, TX) was used to evaluate intraobserver agreement in the assessments on the confidence scale and to test whether the areas under ROC curves related to 100%, 200% and 400% were all equal.

Results

Table 1 shows the intraobserver agreement analysis for diagnosis of the periodontal bone defect using kappa value (κ), and its confidence interval (95% CI) for 100%, 200% and 400% zoomed digital image.

According to the kappa values, $\kappa = 0.48$, $\kappa = 0.54$ and $\kappa = 0.43$, respectively, for 100%, 200% and 400% zoomed digital images, the strength of agreement was considered as moderate. Considering the results of intraobserver agreement by 95% CI, there were no statistical significant differences for the diagnostic performance using 100% (0.32–0.64), 200% (0.38–0.70) and 400% (0.29–0.57) zoomed digital images.

The accuracy of zoomed digital image can be seen in Figure 2, using the ROC curves for the different zooming levels. In addition, Table 2 reports summary statistics and provides a test for the equality of the areas under the curves.

The areas under the ROC curve for 100%, 200%, and 400% zoomed digital images were 0.8611 (95% CI: 0.7660–0.9562), 0.8600 (95% CI: 0.7659–0.9540), and

Table 1 Observed agreement (p_o), expected agreement (p_e) and kappa statistic by point (κ) and by 95% confidence interval (95% CI) according to diagnosis of periodontal bone defects at three levels of zooming

Zooming	p_o	p_e	κ	95% CI
100%	0.65	0.33	0.48	0.32–0.64
200%	0.68	0.31	0.54	0.38–0.70
400%	0.58	0.26	0.43	0.29–0.57

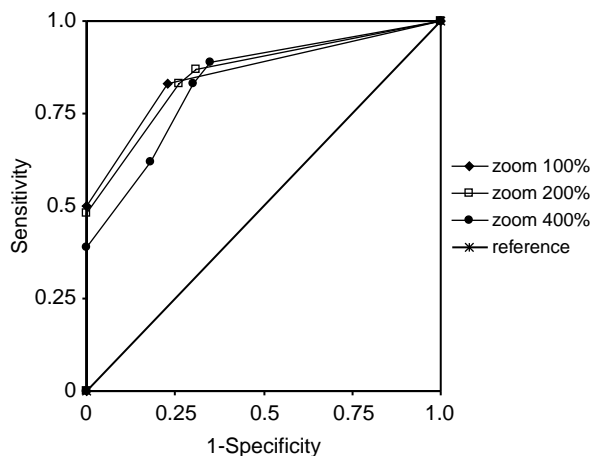


Figure 2 Receiver operating characteristic (ROC) curves for 100%, 200% and 400% zoomed digital images

Table 2 100%, 200% and 400% zooming images and area under receiver operating characteristic (ROC) curves with 95% confidence interval (95% CI)

Zooming	Observations	ROC area	Standard error	95% CI
100%	60	0.8611	0.0485	0.7660–0.9562
200%	60	0.8600	0.0480	0.7659–0.9540
400%	60	0.8368	0.0522	0.7346–0.9390

χ^2 -test (2) = 0.34; prob > χ^2 = 0.8440

0.8368 (95% CI: 0.7346–0.93903), respectively; the χ^2 -test yielded a probability of 0.8440, suggesting that there were no significant differences in the areas under the ROC curves.

Discussion

The results of this study showed a moderate intraobserver agreement for 100%, 200% and 400% zoomed digital images, which could be explained by the limitations of pig anatomical landmarks such as foramen and canals with similar shape as the periodontal bone defect. The moderate agreement values can be an acceptable finding considering this experimental model.

Initially the 804% zoomed digital images were included in the study, but the same classification (uncertain) was reached for each one of the defect sizes, on two different occasions, leading to a perfect agreement because the observer was not able to define the lesions' limit. This zooming was not included in the results because it is a non-useful magnification for the clinical task, thus 400% was considered the upper limit of image zooming.

In a previous study about caries lesions a positive relationship between increased zooming and improvement of diagnostic efficacy was observed with an upper limit of zoomed digital image of $4 \times$.⁹ This finding was similar to our results, although another study also determined the upper limit of zoomed digital image to be $12 \times$,¹³ greater than the results of this study. The comparison between the present study with these papers is limited, however, because they are related to different tasks and the software used for capture and imaging interpretation is also different. When the images are interpreted in different digital systems it is useful to know the software zooming scale.

Regarding accuracy, the results showed that different levels of zooming had similar performances in the detection of periodontal bone defects. The comparative analysis of our results with other papers has been impaired because there are no solid studies that carry out an analysis of the influence of different zooming in detecting periodontal bone defects. Other studies have shown that periodontal bone defects can be detected when there is 30–50% of the mineral bone loss.³ Thus, small percentages of mineral bone loss cannot be detected by zoomed digital images. On the other hand, in the present paper the simulated lesions were done with round bur and the biggest sizes burs (2.0 mm and 3.0 mm) probably removed the buccal cortical plate and reached the trabecular bone. This fact could explain the detection of the bone defects.

It has been reported that although the zoomed digital image can facilitate the radiographic interpretation, this tool does not add any information.¹² We agree with this statement based on our results, which presented the same areas under ROC curves for 100%, 200% and 400% zoomed digital images.

Another relevant aspect is that the radiographic interpretation of artificial lesions with sharp edges does not correspond to the natural bone loss, leading to a limitation of this study. Further studies are suggested to increase the understanding of zoomed digital images in cortical and trabecular bone.

In conclusion, a moderate intraobserver agreement was observed in the classification of periodontal bone defect

and the 100%, 200% and 400% zoomed digital images presented similar performances in the detection of periodontal bone defects.

Acknowledgments

We would like to thank CAPES (Coordenação de Aperfeiçoamento de Pessoal de Nível Superior) for the fellowship.

References

1. Mol A. Imaging methods in periodontology. *Periodontology* 2000; **34**: 34–48.
2. Shrout MK, Jett S, Mailhot JM, Potter BJ, Borke JL, Hildebolt CF. Digital image analysis of cadaver mandibular trabecular bone patterns. *J Periodontol* 2003; **74**: 1342–1347.
3. Jeffcoat MK, Page R, Reddy M, Wannawisute A, Waite P, Palcanis K, et al. Use of digital radiography to demonstrate the potential of naproxen as an adjunct in the treatment of rapidly progressive periodontitis. *J Periodont Res* 1991; **26**: 415–421.
4. Borg E, Attaelmanan A, Gröndahl HG. Subjective image quality of solid state and photostimulable phosphor systems for digital intraoral radiography. *Dentomaxillofac Radiol* 2000; **29**: 70–75.
5. Wenzel A, Gröndahl HG. Direct digital radiography in the dental office. *Int Dent J* 1995; **45**: 27–34.
6. White SC, Yoon DC, Tetradis S. Digital radiography in dentistry: What it should do for you. *CDA* 1999; **27**: 942–952.
7. Eickholz P, Riess T, Lenhard M, Hassfeld S, Staechle HJ. Digital radiography of interproximal bone loss; accuracy of different filters. *J Clin Periodontol* 1999; **26**: 294–300.
8. Versteeg CH, Sanderink GCH, Lobach SR, van der Stelt PF. Reduction in size of digital images: does it lead to less detectability or loss of diagnostic information? *Dentomaxillofac Radiol* 1998; **27**: 93–96.
9. Scaf G, Kantor ML, Walsh SJ. Effect of magnification on caries detection with RadioVisioGraphy (RVG). *J Dent Res* 1993; **72**: 255 (Abstr 1217).
10. Svanaes DB, Møystad A, Risnes S, Larheim TA, Gröndahl HG. Intraoral storage phosphor radiography for approximal caries detection and effect of image magnification: comparison with conventional radiography. *Oral Surg Oral Med Oral Pathol Oral Radiol Endod* 1996; **82**: 94–100.
11. Ellingsen MA, Harrington GW, Hollender LG. Radiovisiography versus conventional radiography for detection of small instruments in endodontic length determination. Part 1. In vitro evaluation. *J Endod* 1995; **21**: 326–331.
12. Kositbowornchai S, Sikram S, Nuansakul R, Thinkhamrop B. Root fracture detection on digital images: effect of the zoom function. *Dent Traumatol* 2003; **19**: 154–159.
13. Møystad A, Svanaes DB, Larheim TA, Gröndahl HG. Effect of image magnification of digitized bitewing radiographs on approximal caries detection: an in vitro study. *Dentomaxillofac Radiol* 1995; **24**: 255–259.
14. Stassinakis A, Brägger U, Stojanovic M, Bürgin W, Lussi A, Lang NP. Accuracy in detecting bone lesions in vitro with conventional and subtracted direct digital imaging. *Dentomaxillofac Radiol* 1995; **24**: 232–237.
15. CDR – Computed Dental Radiography. Schick Technologies Inc. – user manual and installation guide.
16. Fleiss JL, Cohen J. Large sample standard errors of Kappa and weighted Kappa. *Psychological Bull* 1969; **72**: 323–327.
17. Landis JR, Koch GG. The measurement of observer agreement for categorical data. *Biometrics* 1977; **33**: 159–174.
18. DeLong ER, DeLong DM, Clarke-Pearson DL. Comparing the areas under two or more correlated receiver operating curves: A nonparametric approach. *Biometrics* 1988; **44**: 837–845.